Changes in the Kinetics and Emission Spectrum on Mutation of the Chromophore-Binding Platform in *Vibrio harveyi* Luciferase†

Leo Yen-Cheng Lin, Rose Szittner, Romy Friedman, and Edward A. Meighen*

Department of Biochemistry, McGill University, 3655 Promenade Sir William Osler, Montreal, Quebec, Canada H3G 1Y6

Received October 23, 2003

ABSTRACT: The recently proposed model for the bacteria luciferase−flavin mononucleotide complex identifies a number of critical intermolecular interactions that define a binding platform for the isoalloxazine ring of flavin [Lin, L. Y., Sulea, T., Szittner, R., Vassilyev, V., Purisima, E. O., and Meighen, E. A. (2001) *Protein Sci. 10,* 1563−1571]. A key interaction involving van der Waals contact between the isopropyl side chain of αVal173 and the 7,8-dimethyl benzene plane of the isoalloxazine chromophore represents an important target to test the validity of the proposed model. Here, structure−function analysis of luciferase variants carrying single point mutations at position α173 have verified the functional layout of the active site architecture and implicated this site directly in flavin binding. Moreover, a decrease in the stability of the enzyme-bound C4a-hydroperoxyflavin intermediate in the mutants could account for changes in saturation with the fatty aldehyde substrate. A predicted red-shift on mutation of position α173 to increase its polarity confirmed that αVal173 was an integral component of the chromophore-binding microenvironment. Introduction of mutations in residues that contact the pyrimidine plane of the isoalloxazine chromophore (αA75G/C106V) into the αV173A, αV173C, αV173T, and αV173S mutants led to the retention of high levels of enzyme activity (10−40% of wild type) and further red-shifted the emission spectra in the triple mutants. The additivity of the mutation-induced red-shifts in the emission wavelength spectrum provides the basis toward engineering luciferase variants that emit different light colors with the proposed flavin−luciferase model complex as a design reference.

Bacterial luciferase, which consists of two homologous subunits (α and *β*), catalyzes the emission of blue-green light (λ_{MAX} ∼490 nm) in the oxidation−reduction reaction that involves $FMNH_2$, fatty aldehyde, and molecular oxygen as substrates. The structure of the luciferase from *Vibrio harveyi* has been determined by X-ray crystallography, and the structure has revealed a multitude of possible enzyme−substrate interactions with different residues in the active site (*1*, *2*). However, in the absence of the actual substrate-binding coordinates in the crystal structure, these substrate-binding modes have only been inferred based on the protein structural features that would mediate binding. The active site of bacterial luciferase lies within the central cavity of the $(\beta/\alpha)_8$ barrel architecture of the α subunit near a number of amino acid residues implicated in controlling various aspects of the reaction (*3*−*8*). The position of an electron dense inorganic phosphate ion corresponding to the anchoring site for the phosphate group of $FMNH_2$ has been identified in this active site (*1*, *7*, *9*). By combining the proposed phosphate binding location and the chain length requirement of flavin substrates (*10*) as the structural constraints in molecular modeling, we have positioned the flavin mononucleotide into the active site of the luciferase crystal structure (*9*). In the proposed model, the *re*-face of the flavin chromophore clings to a flat molecular surface that is created by the side chains of αAla75, αCys106, and αVal173 with the pyrimidine and the 7,8-dimethyl benzene groups of the flavin chromophore abutting the side chains of αCys106 and αVal173, respectively (*9*). Previously, we have shown that a Cys → Val mutation at position α106 induces small red-shifts in the emission wavelength spectrum (*8*). Addition of the complementary Ala → Gly mutation at position α75 is required to prevent the steric overcrowding of the side chains of αAla75 and αVal106 and maintain the functional efficiency of luciferase (*8*). On the basis of the proposed model structure, we carried out structure−function analysis to verify that αVal173 is an integral component of the structural epitope mediating substrate−enzyme interactions in the predicted chromophore-binding site of bacterial luciferase. In this investigation, a number of mutations of αVal173 were constructed that affect the color of bioluminescence emission and/or the reaction kinetics of luciferase catalysis. Furthermore, incorporation of the αA75G/C106V double mutation into mutants of αVal173 resulted in even larger red-shifts in the emission spectra of bacterial luciferase. The results presented herein not only support the validity of the proposed flavin−luciferase complex model specifying these structural interactions but also suggest that phenotypically desirable bacterial luciferases with different emission colors can be engineered through additive combinations of mutations.

EXPERIMENTAL PROCEDURES

Chemicals. The concentration of flavin mononucleotide (FMN) purchased from Sigma was determined using the

† Supported by Grant MT4314 from the Canadian Institutes of Health Research (CIHR). L.Y.-C.L. is the recipient of the Natural Science and Engineering Research Council of Canada−Canada Graduate Scholarship (NSERC-CGS).

* To whom correspondence should be addressed. Tel: (514) 398-7272. Fax: (514) 398-7384. E-mail: Edward.Meighen@Mcgill.ca.

10.1021/bi030227h CCC: $27.50
Published on Web 02/27/2004

molar extinction coefficient of 12200 M^{-1} cm^{-1} at 450 nm. β-Mercaptoethanol was also purchased from Sigma. The phosphate buffer solution (pH 7.0) was prepared by mixing appropriate amounts of NaH_2PO_4 and K_2HPO_4 purchased from Baker. Sodium dithionite was purchased from Fisher. Octanal, nonanal, decanal, undecanal, and dodecanal were from Aldrich. Bovine serum albumin (BSA) fraction V was obtained from Roche Diagnostics Corp. The 5% platinum on alumina powder was purchased from Pfaltz & Bauer, Inc.

Site-Directed Mutagenesis. The *V. harveyi lux*AB gene in M13 was mutated using the Muta-Gene M13 In Vitro Mutagenesis kit from Bio-Rad. The codon for valine (GTC) at position α173 was changed to asparagine (AAC), leucine (CTG), alanine (GCT), serine (AGC), phenylalanine (TTT), threonine (ACA), isoleucine (ATT), cysteine (TGT), histidine (CAT), and aspartate (GAT). The mutated codons were confirmed by DNA sequencing using the Sequenase DNA Sequencing kit (version 2) from U.S. Biochemical. The mutated *lux*AB cDNA excised from M13 was ligated to the pT7-5 expression vector, and the sequence was reconfirmed as described previously.

Expression and Enzyme Purification. Each of the pT7-5 plasmids containing the mutated *V. harveyi lux*AB gene was expressed in *Escherichia coli* BL21, whose chromosomal DNA encodes the IPTG (isopropyl β-D-thiogalactopyranoside)-inducible T7 RNA polymerase. The cells harboring the plasmid were grown in the Terrific Broth containing 50 μg/mL ampicillin at 30 °C, and IPTG was added to a final concentration of 1.2 mM when the cell density reached an OD_{660} of 1.2−1.3. Following the induction with IPTG, the cell culture was allowed to grow for 1−2 h before luciferase extraction took place. Cells were harvested, centrifuged, and resuspended in 5% of the original culture volume of 1 mM phosphate buffer (pH 7.0) containing 5 mM EDTA and 10 mM β-mercaptoethanol before lysis by ultrasonication. After lysis, the cell debris was removed by centrifugation, and the phosphate concentration of the supernatant containing the extracted luciferases was adjusted to 100 mM (pH 7.0). Protein purification was performed on the supernatant according to previous methods (*11*). Protein concentrations were first estimated using the Bio-Rad protein determination kit with BSA (bovin serum albumin) as a standard. More accurate protein concentrations were determined spectrophotometrically using the protein extinction coefficient calculated using Gill and von Hippel's method (*12*).

Measurement of Luminescence Intensity. Three different techniques were employed, depending on the kinetic parameter in question. They are the standard flavin injection assay (*13*), the sodium dithionite assay (*14*), and the double-injection assay (*10*). The activities of luciferases, including mutants and the wild type, were measured using the standard flavin injection assay, in which 1 mL of the platinum−hydrogen gas-reduced 50 μM flavin mononucleotide ($FMNH_2$)[1] was rapidly injected into the 1 mL assay buffer [50 mM phosphate and 0.2% bovine serum albumin (pH 7.0)] containing aldehyde [0.001% (v/v) for measuring the specific activities and the rates of luminescence decay] and luciferase. The rate of luminescence decay ($=0.69/t^1/_2$) was determined from the time ($t^1/_2$) it took for the light intensity to decay from 80 to 40% of the maximum light intensity. The binding affinity of luciferase for $FMNH_2$ ($K_D = K_M$) was determined using the dithionite assay, in which 1 mL of 0.1% decanal solution (v/v in water) was injected into the 1 mL assay mixture (pH 7.0) containing luciferase, FMN, 0.2−0.6 mg of sodium dithionite, 0.025 M β-mercaptoethanol, and 50 mM phosphate. The stability of the luciferase bound C4a-hydroperoxyflavin intermediate was determined with the double-injection assay, in which 1 mL of the platinum−hydrogen gas-reduced 50 μM flavin mononucleotide was first injected into the 1 mL assay mixture (pH 7.0) containing luciferase, 0.2% bovine serum albumin, and 50 mM phosphate, followed by the injection of 1 mL of 0.1% decanal (v/v in water) at different time points. As the luminescence intensity registered by the photomultiplier photometer (*15*) is constantly recorded by the computer at a 5 ms interval, the time difference between the rapid mixing of the first $FMNH_2$ injection and the second decanal injection is measured at the precision of milliseconds allowing the decay rate of the unstable C4a−hydroperoxyflavin intermediate (i.e., 200 ms $\leq t^1/_2 \leq$ 1 s) to be determined accurately.

Luminescence Wavelength Scan. The emission wavelength spectra were scanned with a Hitachi F-3010 spectrofluorometer using the following settings: internal shutter closed to block the xenon lamp from exciting the sample, wavelength dispersion for emission band-pass set at 5 nm, scan speed of 600 nm/min between 420 and 550 nm, and sample chamber temperature controlled at 23 °C. The coupled assay described by Hastings et al. (*13*) was modified by the addition of the Type XXIII *Leuconostoc mesenteroides* glucose-6-phosphate dehydrogenase (purchased from Sigma) and its substrates. Luminescence was generated continuously from the mixture containing 50 mM phosphate buffer (pH 7.0), 0.2% bovine serum albumin, 5 mM β-mercaptoethanol, 0.1 mM decanal, 5 μM FMN, 1 mM β-nicotinamide adenine dinucleotide (NAD), 5 mM glucose-6-phosphate, 0.2 unit of the Type XXIII *L. mesenteroides* glucose-6-phosphate dehydrogenase, approximately 50 μg of ≥90% pure luciferase (for mutants with low quantum efficiency, approximately 2−3 mg of the purified luciferase was used to produce luminescence with high signal-to-noise ratio), and a fixed amount of partially purified *V. harveyi* FMN reductase with both NADH- and NADPH-dependent activities (*16*). The reaction mixture was mixed with an in-curvet magnetic stir bar using the magnetic stirring device built into the spectrofluorometer. Light intensity remained constant over the period of wavelength scanning.

RESULTS

Single-Turnover Assay. The mechanism of the bacterial luciferase catalyzed reaction (Figure 1) outlines the sequence of key intermediates that intervene between substrates and products (*17*, *18*). Along the reaction pathway, the stable EFO intermediate, which is formed upon the addition of molecular oxygen (O_2) to the luciferase bound flavin substrate (EF), interacts reversibly with aldehyde (A) to form the EFOA enzyme−substrate complex that will decay with a rate constant, k_L, to produce light. However, in the absence of aldehyde, the enzyme bound C4a-hydroperoxyflavin intermediate (EFO) spontaneously decays through a nonproductive dark pathway with a rate constant, k_D, and decomposes into the oxidized flavin and hydrogen peroxide,

[1] Abbreviations: $FMNH_2$, reduced flavin mononucleotide.

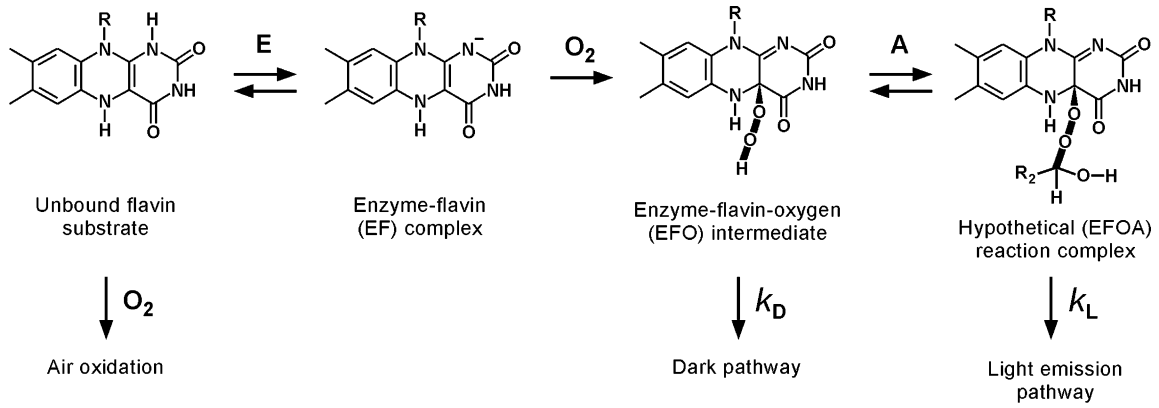

FIGURE 1: Key intermediates in the bacterial luciferase catalyzed reaction.

Table 1: Relative Specific Acitivities of Luciferase Mutants as Compared to Wild-Type Luciferase with Different Aldehydes[a]

	aldehyde				
mutants	octanal	nonanal	decanal	undecanal	dodecanal
V173A	10	10	20	20	20
V173C	10	10	10	20	20
V173S	10	10	10	10	10
V173T	30	40	70	50	50
wild type	100	100	100	100	100
V173I	50	60	50	60	50
V173L	1	1	1	1	1
V173N	1	1	2	1	2
V173D	0.01	0.01	0.03	0.02	0.03
V173F	0.001	0.001	0.002	0.001	0.001
V173H	0.0002	0.0002	0.0003	0.0003	0.0004
A75G/C106V	60	80	50	80	80
A75G/C106V/V173A	10	10	20	30	30
A75G/C106V/V173C	20	20	30	40	40
A75G/C106V/V173S	5	5	10	10	10
A75G/C106V/V173T	10	10	20	10	20

[a] The specific activities of wild-type luciferase with 0.001% (v/v) octanal, nonanal, decanal, undecanal, and dodecanal were 4.8×10^{13}, 3.5×10^{14}, 3.3×10^{14}, 5.5×10^{13}, and 4.2×10^{13} quanta s^{-1} mg^{-1}, respectively.

Table 2: Rates of Luminescence Decay of Wild-Type and Mutant Luciferases with Different Aldehydes[a]

	k_T (s^{-1})				
mutants	octanal	nonanal	decanal	undecanal	dodecanal
V173A	0.31	0.31	0.35	0.24	0.083
V173C	0.33	0.41	0.52	0.24	0.088
V173S	1.3	1.3	1.4	0.93	0.31
V173T	0.26	0.41	0.47	0.17	0.067
wild-type	0.045	0.32	0.26	0.057	0.047
V173I	0.037	0.24	0.27	0.045	0.035
V173L	0.86	0.87	0.71	0.45	0.12
V173N	2.0	2.8	2.6	1.5	0.57
V173D	1.6	2.7	2.2	0.99	0.49
V173F	0.75	1.0	1.3	0.64	0.21
V173H	0.82	0.91	0.79	0.53	0.23
A75G/C106V	0.095	0.32	0.33	0.070	0.048
A75G/C106V/V173A	0.36	0.29	0.27	0.20	0.095
A75G/C106V/V173C	0.64	0.48	0.39	0.37	0.17
A75G/C106V/V173S	2.3	1.7	1.3	1.0	0.48
A75G/C106V/V173T	0.23	0.53	0.55	0.14	0.075

[a] The decay rate ($k_T = \ln 2/t_{1/2}$) was calculated from the time interval for luminescence to decay from 80 to 40% of maximum light intensity at 0.001% (v/v) aldehyde.

yielding no light. The enzyme kinetics of the bacterial luciferase-catalyzed reaction is unique in that the decay of the EFO intermediate through either the light or the dark pathway is much slower than the rapid chemical oxidation of the unbound flavin substrate. Consequently, bacterial luciferase catalyzes only one cycle of reaction upon the rapid mixing of the enzyme and substrates ($FMNH_2$, O_2, and fatty aldehyde). In the single turnover reaction, the maximum light intensity (I_0) gives the activity of luciferase, and the rate of luminescence decay (k_T) reflects the duration of a single reaction cycle. Integration of the light intensity produced over a single cycle gives the amount of light per enzyme turnover and reflects the quantum yield.

Functional Efficiencies of α*Val173 Mutants.* A key residue proposed to directly interact with the isoalloxazine group of flavin is αVal173 (*9*). Replacement of Val by one of the other natural amino acids causes changes in the side chain size, shape, and/or polarity. Table 1 lists the 10 mutations chosen for replacement of αVal173. Comparison of the enzyme activity (Table 1), luminescence decay rate (Table 2), and quantum yield (Table 3) shows that at position α173, a compact amino acid possessing a branched tertiary β-carbon in the side chain (i.e., Thr, Val, and Ile) is preferred for the efficient production of light. Deviation from these stringent structural specifications results in the reduction of enzyme activity, reaction duration, and quantum yield. These data also show that the luciferases mutants, in which αVal173 is replaced with a larger amino acid (i.e., Leu, Asn, Asp, His, Phe), suffer the most significant reductions in functional efficiency. In contrast, replacement of αVal173 with a residue that possesses a small side chain (i.e., Ala, Cys, Ser) or a structure similar to Val (i.e., Thr and Ile) maintains the functional efficiency of luciferase at a reasonable level. As the efficiency of light emission is dependent on several kinetic parameters that determine the binding affinities and intermediate stabilities along the reaction pathway, the causes for the loss of functional efficiency in these mutants were investigated for alterations of these kinetic properties.

Binding of $FMNH_2$. The $FMNH_2$ binding affinity of luciferase accounts for the ability of luciferase to form a functional EF (enzyme:$FMNH_2$) complex in the initial step of the reaction pathway (Figure 1). The markedly weakened $FMNH_2$ binding affinities associated with the αV173L,

Table 3: Relative Luminescence Light Yield (%) of Luciferase Mutants[a]

	aldehyde				
mutants	octanal	nonanal	decanal	undecanal	dodecanal
V173A	1.5	10	15	5	15
V173C	1.5	10	5	5	10
V173S	0.2	1.5	2	0.5	2
V173T	5	30	40	15	40
wild-type	100	100	100	100	100
V173I	60	70	50	70	60
V173L	0.03	0.2	0.3	0.07	0.4
V173N	0.01	0.1	0.2	0.03	0.2
V173D	0.0002	0.002	0.003	0.001	0.003
V173F	0.00008	0.0004	0.0003	0.0001	0.0003
V173H	0.000009	0.00005	0.0001	0.00003	0.00008
A75G/C106V	30	80	40	60	80
A75G/C106V/V173A	2	10	20	10	20
A75G/C106V/V173C	1	10	20	10	10
A75G/C106V/V173S	0.05	0.5	1.5	0.5	1
A75G/C106V/V173T	2	10	10	5	10

[a] The light yields were calculated by multiplying the specific activities (Table 1) and the $t_{1/2}$ (Table 2) and were expressed as % relative to wild-type luciferase for the respective aldehyde.

Table 4: Substrate Binding Constants of Luciferase Mutants for $FMNH_2$[a]

mutants	K_M (M) × 10^7	mutants	K_M (M) × 10^7
V173A	6	V173D[b]	≫1000
V173C	4	V173F	≥1000
V173S	80		
V173T	30	A75G/C106V	20
wild type	6	A75G/C106V/V173A	20
V173I	4	A75G/C106V/V173C	4
V173L	≥1000	A75G/C106V/V173S	100
V173N	≥1000	A75G/C106V/V173T	200

[a] The Michaelis−Menten constants of the bacterial luciferases for FMNH2 substrate, K_M, are determined with the dithionite assay described in Experimental Procedures. [b] The activity of the V173D mutant increases in a straight linear relationship as the $FMNH_2$ concentration is increased up to 600 μM. In contrast to the other luciferase mutants, the inability to saturate the V173D mutant in the dithionite assay indicates that V173D has the lowest efficiency in forming the functional EF complex. The activity of αV173H was too low to determine the K_M.

αV173N, αV173D, or αV173F mutations (Table 4) explain the severe losses of their functional efficiencies and show that the augmentation of the side chain size at position α173 significantly impedes the functional association of luciferase with $FMNH_2$. In addition, a weakening of the $FMNH_2$ binding affinity is also associated with an increase in side chain polarity at position α173 (i.e., Thr and Ser), emphasizing that the replacement of αVal173 with compact and hydrophobic side chains at position α173 (i.e., Ala, Cys, Ile) is important to maintain the strong association of luciferase with $FMNH_2$.

It is noteworthy that the preference for an amino acid residue with a compact side chain at position α173 parallels a similar structural requirement for the side chain at position α106 that is immediately adjacent to position α173 in the three-dimensional structure of bacterial luciferase (*2*). Paquatte and Tu (*19*) have discovered that methyl *p*-nitrobenzene sulfonate, which selectively methylates the thiol group of αCys106, inactivates luciferase demonstrating the stringency in the extension of side chain at position α106. In our proposed enzyme−flavin model, the parallel aligned side chains of αCys106 and αVal173 interact directly with the isoalloxazine chromophore (*9*). In addition, the compact, hydrophobic side chain at position α173 (Val) together with the cysteinyl side chain at position α106 forms a unique patch of amphipathic surface, complementing the isoalloxazine chromophore in the proposed model (Figure 2). The requirement for a nonpolar microenvironment at position α173 for flavin binding is in agreement with the predicted van der Waals contact that is established between the isopropyl side chain of αVal173 and the 7,8-dimethyl benzene moiety of the flavin chromophore (*9*). The hydrophobic nature of the protein microenvironment that embraces the 7,8-dimethylbenzene moiety of flavin in the wild type *V. harveyi* luciferase has been previously recognized by nuclear magnetic resonance (*20*, *21*). Furthermore, the nonprolyl *cis*-peptide linkage of αAla74−Ala75, which is in juxtaposition to αVal173 and αCys106, establishes hydrogen bonds to the C4 carbonyl oxygen and the N5 hydrogen of the isoalloxazine ring in the proposed model (Figure 2). Because the extension of the side chain at positions α106 or α173 into the active site cavity would interfere with the molecular coordination between the isoalloxazine group of $FMNH_2$ and the protruding *cis*-amide linkage of αAla 74−αAla 75 (Figure 2), these results would indirectly support the speculated role of the *cis*-amide linkage of αAla 74−αAla 75 in substrate binding and possibly reaction catalysis (*8*).

C4a-Hydroperoxyflavin Intermediate Stability. In the absence of aldehyde substrate (A), the enzyme bound C4ahydroperoxyflavin intermediate (EFO) spontaneously decays through the dark pathway, yielding no light (Figure 1). By injecting aldehyde (A) at different time points after the formation of the EFO ternary complex, the level of active C4a−hydroperoxyflavin intermediate and its decay rate in the dark pathway can be determined. Comparison of the decomposition rate (k_D) of the C4a−hydroperoxyflavin intermediate reveals that replacement of αV173 by most amino acids tested (except Ile) significantly (4−30-fold) destabilizes the EFO intermediate (Table 5). The mutational effects on the stability of the EFO intermediate differ to some extent from their effects on enzyme activity and $FMNH_2$ binding affinity where incorporation of amino acids larger than Val (i.e., αV173L, αV173N, and αV173D) nearly abolish the enzyme function. In contrast, these mutations (i.e., αV173L, αV173N, and αV173D) alter the rate of EFO decay to levels that are similar to substitution with small, polar amino acids (i.e., αV173T and αV173S).

Furthermore, it is relevant that the destabilization of the EFO ternary complex by mutation at position α173 also occurs in luciferase variants mutated at position α106 (i.e., αC106A, αC106S, and αC106V) (*22*, *23*). As both residues are proposed to bind directly to the amphipathic isoalloxazine chromophore in the active site (Figure 2), the more rapid EFO decay associated with these specific mutations suggests that the alteration in the complementary nature between the flavin chromophore and the contacting side chains at position α106 and α173 contributes to the kinetic destabilization of the C4a−hydroperoxyflavin intermediate.

Aldehyde Binding. Figure 1 shows that through the reversible binding interaction between the aldehyde and the EFO intermediate in the formation of the EFOA reaction

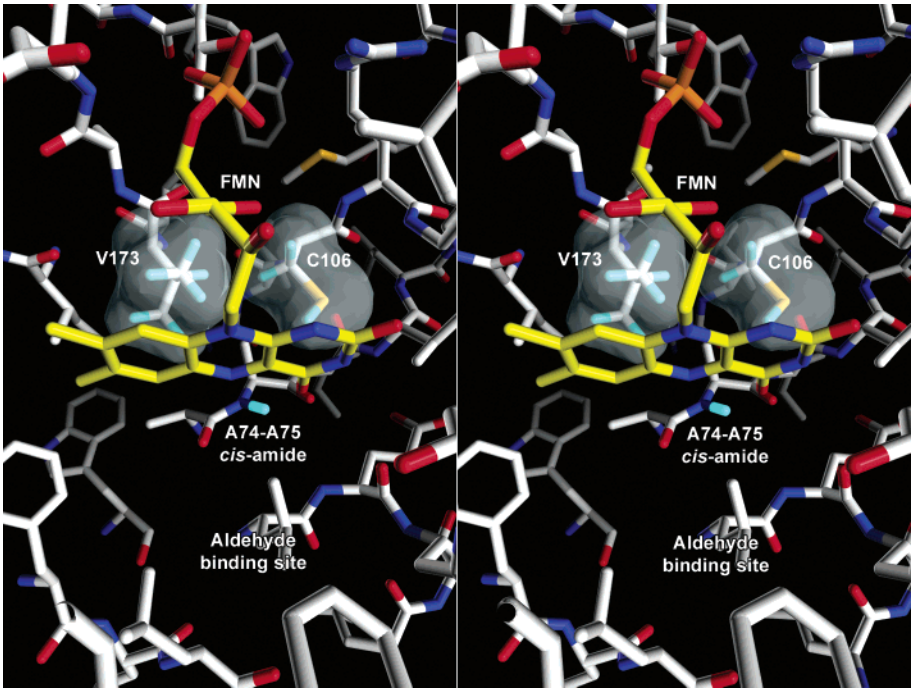

FIGURE 2: Stereoview of the proposed FMN binding site. Molecular surfaces of αVal173 and αCys106 in juxtaposition show that both side chains are extended in uni-parallel direction toward the proposed isoalloxazine chromophore. The extension of valine and cysteine side chains from position α173 and α106 provides optimal displacement abutting the planar isoalloxazine chromophore directly above the αAla74−αAla75 *cis*-amide bond. The cavity space on the *si*-face of the isoalloxazine chromophore is the aldehyde binding site outlined in the proposed functional layout of the active site architecture. Hydrogen atoms other than those of αVal173, αCys106, and the backbone amide NH of αAla75 were omitted for clarity.

Table 5: Rate Constants of the Enzyme−Flavin−Oxygen (EFO) Intermediate Decay through the Dark Pathway[a]

mutants	k_D (s^{-1})	mutants	k_D (s^{-1})
V173A	0.71	V173D	2.8
V173C	0.51	V173F[b]	n/a
V173S	3.4		
V173T	1.0	A75G/C106V	0.27
Ww	0.12	A75G/C106V/V173A	0.86
V173I	0.15	A75G/C106V/V173C	0.78
V173L	1.2	A75G/C106V/V173S	5.1
V173N	3.5	A75G/C106V/V173T	1.6

[a] The rate constants of the dark pathways, k_D, in bacterial luciferases are determined with the double injection assay described in Experimental Procedures. [b] Because of the low activity nature of V173F and the rapid EFO decay, a significant level of light intensity could not be detected beyond 200 ms after the initial $FMNH_2$ injection; therefore, the decay pattern could not be accurately determined.

complex, the aldehyde directly competes with the dark pathway for utilization of the luciferase bound C4a−hydroperoxyflavin intermediate. A formulated equation (*24*) that correlates the rate of luminescence decay (k_T) to the rate constants (k_L and k_D) in both light and dark pathways, as well as the aldehyde concentration and the aldehyde dissociation constant ($K_{d(ald)}$), is given next.

$$k_T = (k_L A + k_D K_{d(ald)})/(K_{d(ald)} + A) \quad (1)$$

At low aldehyde concentrations ($A < K_{d(ald)}$), formation of the EFOA enzyme−substrate complex is inefficient, and the EFO intermediate decays primarily through the dark pathway with $k_T \approx k_D$. At high aldehyde concentration ($A > K_{d(ald)}$), the association between the EFO and the aldehyde substrate to form the EFOA complex is favored, and the reaction proceeds primarily through the light emission pathway such that $k_T \approx k_L$.

Determination of the dissociation constant for aldehyde $\{K_{d(ald)} = [EFO][A]/[EFOA]\}$ is complicated by the decay of the EFO and EFOA intermediates through dark and light pathways. As the equilibration between EFO and EFOA intermediates occurs much faster than the decay of intermediates through either the dark or the light pathways, the aldehyde concentration that elicits 50% of the maximum enzyme activity ($[A^*] = K_{M(ald)}$) occurs when the rates of intermediate distribution (EFO and EFOA) through the dark and light pathways are equal, such that k_D [EFO] = k_L [EFOA]. Under this reaction condition, substitution and rearrangement of the previous equations lead to eq 2.

$$K_{M(ald)} = (k_D/k_L)K_{d(ald)} \quad (2)$$

Consequently, the $K_{M(ald)}$ would increase upon destabilization of the EFO intermediate (increase in k_D) for the mutants. The effect of mutation of αVal173 on aldehyde (i.e., decanal) binding (Figure 3) reveals that the increase in $K_{M(ald)}$ is closely correlated with the increase in the rate of EFO decay (k_D) via the dark pathway although the data is complicated by inhibition by aldehyde at higher concentrations. Both the mutants (αV173I and αV173C) with the lowest rates of EFO decay (k_D = 0.15 and 0.5 s^{-1}) and the wild type (k_D = 0.12 s^{-1}) reach maximum light intensity at 25 μM decanal. Mutants (αV173A, αV173T, and αV173L) with an intermediate rate of EFO decay (k_D = 0.7 to 1.2 s^{-1}) require 50 μM decanal for maximum enzyme activity, while mutants (αV173S, αV173N, and αV173D) with a high rate of EFO decay ($k_D \approx 3$ s^{-1} and higher) require at least 100 μM decanal for maximum enzyme activity. Estimation of the dissociation constants for aldehyde binding ($K_{d(ald)}$) using eq 2 indicates that all mutants would have a $K_{d(ald)}$ within 3-fold of that of the wild type showing that the apparent weakening in the

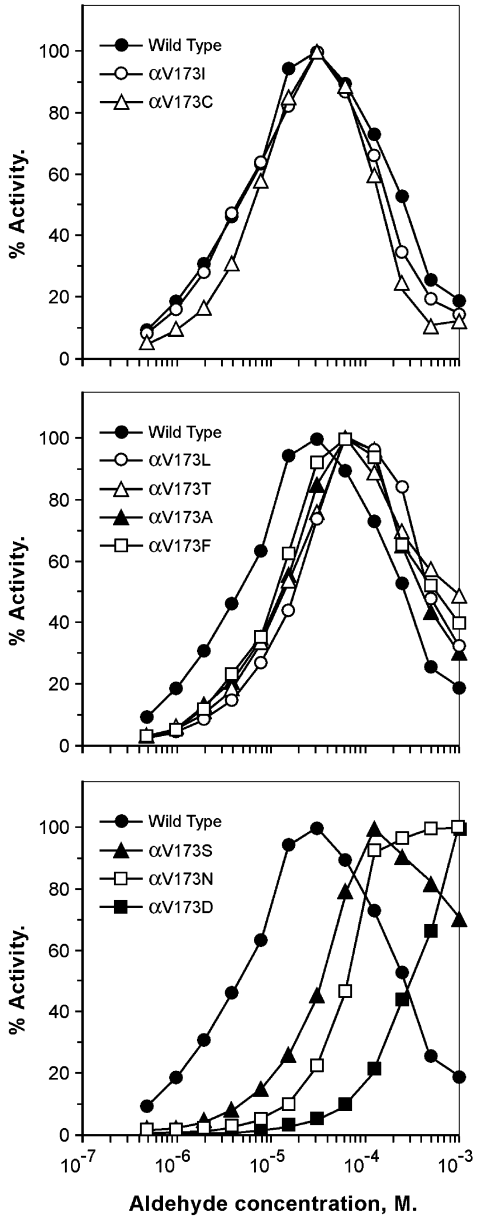

FIGURE 3: Luminescent light intensity as a function of decanal concentration determined for mutant and wild-type luciferases. The % activity on the *y*-axis denotes the percentage of the maximum luminescent light intensity determined for each luciferase. The luminescence intensities of luciferases were determined in 0.2% BSA−50 mM phosphate (pH 7.0) in the standard flavin injection assay.

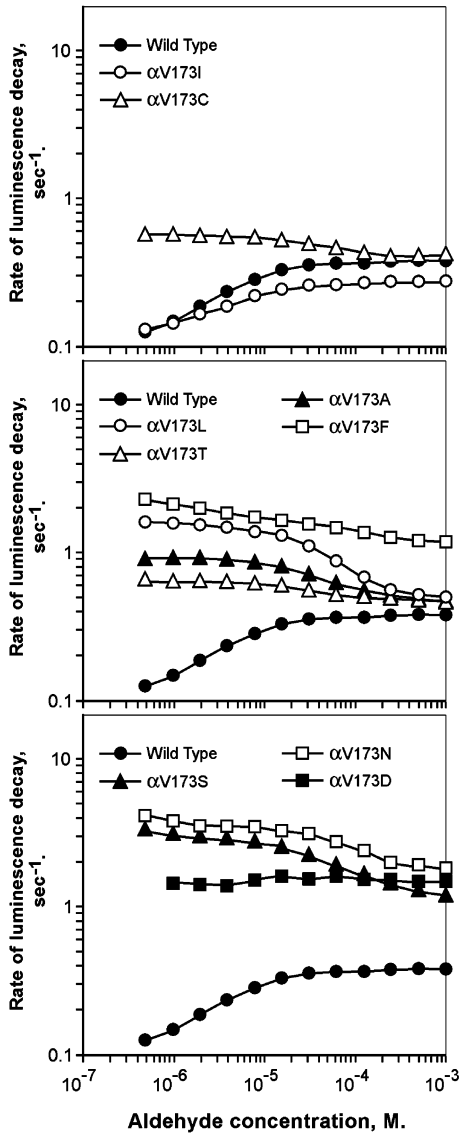

FIGURE 4: Rate of luminescent decay as a function of decanal concentration determined for mutant and wild-type luciferases. The decay rate ($k_T = \ln 2/t_{1/2}$) on the *y*-axis was calculated from the time interval for luminescence to decay from 80 to 40% of maximum light intensity. The luminescence intensities of luciferases were determined in 0.2% BSA-50 mM phosphate (pH 7.0) in the standard flavin injection assay.

aldehyde binding (i.e., higher K_M) is accounted for by increases in k_D and that mutation at αVal173 has little effect on $K_{d(ald)}$.

Figure 4 shows the dependence of the rates of luminescence decay (k_T) on decanal concentration. As predicted by eq 1, the luminescence decay rates (k_T) determined for the luciferases (wild type and mutants) at low aldehyde concentration (<1 μM) are similar to the rates of EFO intermediate decay in the dark pathway (k_D), demonstrating that the destabilization of the EFO intermediate significantly withdraws the EFOA complex toward dissociation in the dark pathway and that in turn contributes to the fast decay of luminescence intensity (k_T) in the single turn-over assay. At high decanal concentration (>100 μM), the rates of luminescence decay (k_T) for the majority of mutants (i.e., αV173I, αV173C, αV173L, αV173A, and αV173T) converge toward that of the wild type (0.4 s^{-1}), suggesting that the alteration in the side chain structure at position α173 does not affect the rate constant in the light emission pathway (k_L). It is noted that the rates of luminescence decay for αV173S, αV173F, αV173N, and αV173D mutants remain high even at high aldehyde concentrations. Although eq 1 predicts that the rate constant in the light emission pathway (k_L) can be estimated from the rate of luminescence decay (k_T) at saturating aldehyde concentration, the high rates of EFO decay ($k_D \sim 3$ s^{-1}) for these mutants coupled with the low solubility of fatty aldehyde may make it difficult to achieve aldehyde saturation under these circumstances. Thus, even high decanal concentrations may not block decay via the dark pathway for these mutants (i.e., αV173S, αV173F, αV173N, and αV173D), and the rates of luminescence decay (k_T) would still be largely influenced by k_D. However, the

possibility of changes in k_L and concomitant effects on aldehyde binding cannot be excluded for these latter mutants.

It is important to note that although mutants with similar rates of EFO decay (k_D) have the same dependence of enzyme activity on aldehyde concentration, these mutants are dramatically different in terms of their specific activities, quantum efficiency, and $FMNH_2$-binding affinity, which arise from deviations from the side chain structure of αVal173. Higher aldehyde concentrations are needed to enforce the formation of the productive EFOA reaction complex if the rate of EFO decay via the nonproductive dark pathway is increased thus causing a shift in the aldehyde binding curve. The dependence of aldehyde binding on the decay rates of the competing dark and light emission pathway is consistent with αVal173 and fatty aldehyde not being in direct contact and on opposite sides of the isoalloxazine plane as depicted in Figure 2 so that the effects of mutation of αVal173 on aldehyde binding is mediated through the flavin. The active site in the three-dimensional structure of bacterial luciferase is a large hollow cavity, in which the luminescence reaction with all three substrates ($FMNH_2$, O_2, and aldehyde) is catalyzed. In the modeling of the luciferase−flavin binary complex, the docking of the proposed flavin mononucleotide model in the active site subsequently revealed a tunnel-shaped cavity next to the *si*-face of the catalytic isoalloxazine chromophore suitable for binding of the fatty aldehyde and molecular oxygen (*9*). In this arrangement, the flavin isoalloxazine plane serves as a divider intervening between the side chains of αVal173 and the aldehyde (Figure 2), and this functional layout of the active site cavity is directly supported by the data from the current mutational analysis of αVal173.

Bioluminescence Spectral Distribution. The color of bacterial bioluminescence corresponding to the energy of the emitted photon can be changed by modification of the structure of the isoalloxazine chromophore (*25*). Modification of the dielectric field in the binding microenvironment of the flavin chromophore in the luminescent reaction should also alter the emission color by perturbing the potential energy of the chemically excited state and/or the stable ground state. To scan the emission spectrum of the purified αVal173 luciferase mutants, an assay system with constant light intensity is needed. This was accomplished by the continual regeneration of $FMNH_2$ with a *V. harveyi* NAD(P)H-dependent FMN reductases (*16*) using d-glucose phosphate as a reservoir of reducing power and the Type XXIII *L. mesenteroides* d-glucose-6-phosphate dehydrogenase to maintain the NADH levels as outlined in Figure 5.

Figure 6 shows that the emission spectra of the mutants that carry a more polar side chain at position α173 are red-shifted to that of the wild type (i.e., αV173T, αV173S, αV173C, αV173D, and αV173N). In contrast, mutants carrying hydrophobic side chains (i.e., αV173I, αV173L, and αV173F) all yield identical emission spectra to that of the wild-type luciferase with αVal173. The only potential exception is αV173A whose spectrum is also red-shifted, perhaps due to an increase of polarity due to incursion of water on substitution by the smaller alanine residue. The presence of a polar side chain at position α173 apparently decreases the probability of the chemically energized chromophore reaching a high energy excited state and/or destabilizes the ground state causing a red-shift in the emission spectra. The absence of any emission spectral shift from the αV173I, αV173L, and αV173F mutants despite their wide differences in activity (0.001−100% including the wild type) and other kinetic properties arising from potential steric interference with flavin clearly indicates that the red-shifted emission spectra of the mutants, which carry a polar side chain at position α173, are solely ascribed to alteration of the electronic nature of the chromophore-binding site. Therefore, changes in the emission spectra of these luciferase variants associated directly with changes in polarity and not with kinetic properties provide a concrete and independent set of evidence for the proximity of αVal173 and the isoalloxazine chromophore as predicted in the luciferase−flavin model (Figure 2).

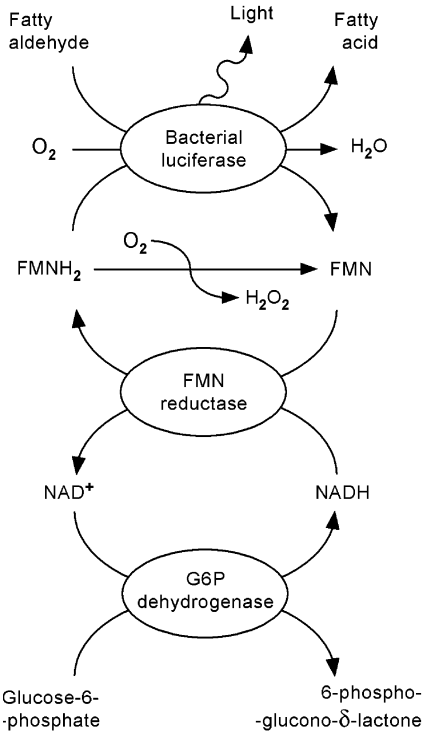

FIGURE 5: Reduction of NAD^+ to NADH, which is catalyzed by the glucose-6-phosphate dehydrogenase, fuels the FMN reductase to regenerate $FMNH_2$. The coupling of these three enzymatic reactions ensures a constant supply of $FMNH_2$ to bacterial luciferase and enables luciferase to produce luminescence over the extended period of time in vitro.

Triple Mutants. Previously, we have shown that the emission spectra of luciferases carrying the αC106V mutation, whose side chain along with αVal173 directly contacts the *re*-face plane of the flavin chromophore (Figure 2), were also red-shifted (*8*). However, the αC106V single mutant has only 1−2% of the wild type enzyme activity and destabilizes the bound C4a−hydroperoxyflavin intermediate (k_D ranges from 4.3 to 13.0 s^{-1}) (*22*, *23*). The debilitation in function is due to a steric clash of the isopropyl group of αVal106 against the methyl side chain of αAla75 as the enzyme activity, and EFO stability can be restored to wild type levels by mutating αAla75 to Gly generating the double mutant, αA75G/C106V (*8*). To maintain high functional efficiency and generate larger shifts in the emission wavelength spectrum, the αA75G/C106V double mutation was combined with the αV173A, αV173T, αV173S, and αV173C mutations, which retain good functional efficiency and also red-shift the emission spectra, to create four triple mutants.

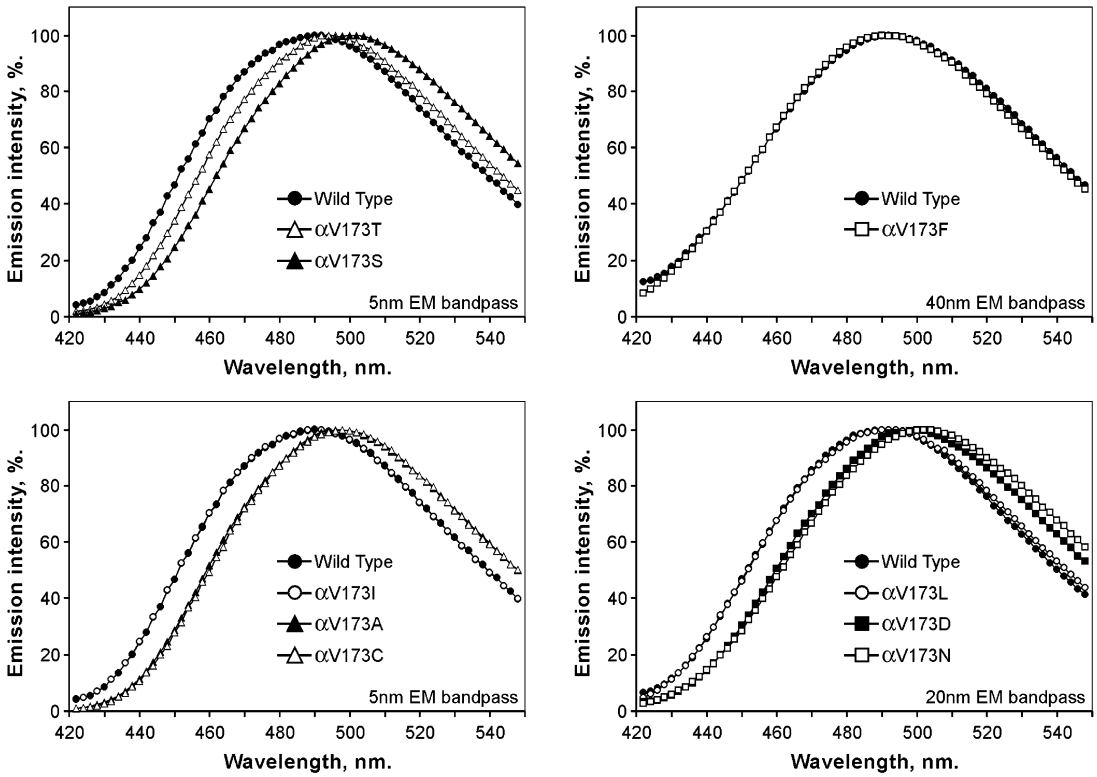

FIGURE 6: Luminescence emission wavelength scans of *V. harveyi* wild-type and mutant luciferases. Mutations of αVal173 with residues possessing either amphipathic or polar side chains red-shifts the emission spectrum. The emission spectra of mutants carrying bulky and hydrophobic side chains at position α173 were identical to that of the wild-type as their scan lines overlap. The emission (EM) band-pass denoted at the bottom right corner of every panel represents the slit width used in the measurement of light intensity produced at every defined wavelength. Mutants with poor activities producing low yields of light intensity were scanned at a much wider slit width to obtain a high signal-to-noise ratio, and in those cases, the emission spectrum of the wild-type was also scanned with a wide slit width for direct comparisons in each panel.

Tables 1−3 (bottom) show that the functional efficiencies of all four triple mutants are reasonably high with the αA75G/C106V/V173A and αA75G/C106V/ V173C triple mutants being more active and the αA75G/C106V/V173T and αA75G/C106V/V173S triple mutants being less active than the corresponding α173 single point mutants. This differential response of the αV173 single mutants may indicate that introduction of the αA75G/C106V double mutation increases the specificity at position α173 for a hydrophobic (Cys/Ala) over a polar (Thr/Ser) side chain as it would be caged in a hydrophobic environment constituted of the side chain of αVal106 in the αA75G/C106V double mutant and the 7,8-dimethyl benzene moiety of the isoalloxazine chromophore.

The EFO stability was relatively unaffected by introducing the αA75G/C106V double mutation with the k_D of all four triple mutants being 1.2−1.6 times that of their respective single point α173 mutants (Table 5). In addition, as predicted by eq 2, aldehyde affinity weakens with a rise in k_D. For the triple mutants containing αS173, αT173, or αC173, in which k_D is 1.5−1.6 times that of the respective single point αV173 mutant, the aldehyde binding curves shift toward higher concentration. While for the αA75G/C106V/V173A triple mutant, whose k_D is only 1.2 times that of the αV173A mutant (Table 5), the apparent dependence of activity on aldehyde concentration remains almost identical to that of αV173A (Figure 7).

It is known that *V. harveyi* wild type luciferase is prone to substrate inhibition at high aldehyde concentrations (*26*). As the mutation of αCys106 alleviates this inhibition (*8*, *22*, *23*), the reactive thiol group of αCys106 has been related to this inhibition (*26*). The lack of substrate inhibition is clearly illustrated in Figure 7 for the αA75G/C106V double mutant and the triple mutants containing Val at position α106 with one major exception. When the αA75G/C106V and αV173C mutations are combined, the inhibition at high aldehyde concentration is regenerated, indicating that a Cys residue at position α173 can also cause this phenotype. Reversible nucleophilic addition of the reactive cysteinyl side chain to the aldehyde carbonyl forming an unstable thiol hemi-acetal is believed to lead to encroachment of the aldehyde into the flavin binding site, preventing the formation of a functional EF complex in the initial phase of the reaction pathway. The ability of αCys173 as well as αCys106 to lead to aldehyde inhibition suggests a close proximity of both residues to the flavin binding site, reinforcing the validity of the proposed model (Figure 2).

In terms of the functional EF (enzyme:$FMNH_2$) complex formation, we have previously shown that the αC106V mutant retains a strong binding affinity toward $FMNH_2$ (K_M = 0.6 μM) (*8*). Incorporation of the αA75G mutation into luciferase weakens the affinity of both αA75G and αA75G/C106V mutants for $FMNH_2$ (K_M = 2−3 μM) (*8*). Table 4 shows that the addition of the αA75G/C106V double mutation to the αV173T or αV173S mutants weakens their $FMNH_2$-binding affinities so that the K_M for $FMNH_2$ of the triple mutants, αA75G/C106V/V173S and αA75G/C106V/V173T, is increased to 10 and 20 μM, respectively. In

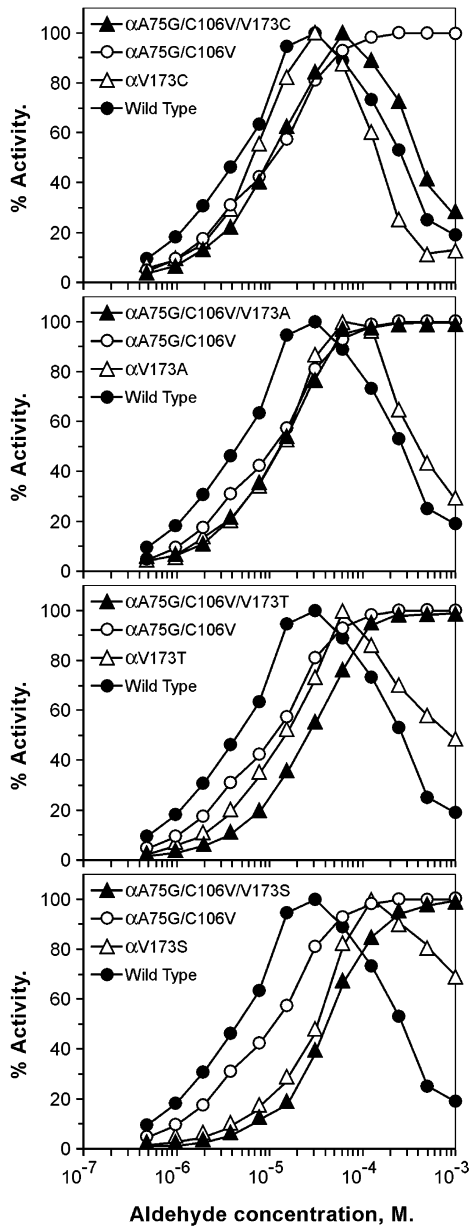

FIGURE 7: Luminescent light intensity as a function of decanal concentration determined for the mutants, wild-type, and αA75G/C106V double mutant. The % activity on the *y*-axis denotes the percentage of the maximum luminescent light intensity determined for each luciferase. The luminescence intensities of luciferases were determined in 0.2% BSA−50 mM phosphate (pH 7.0) in the standard flavin injection assay.

contrast, the $FMNH_2$-binding affinity of the αA75G/C106V/V173A triple mutant remains identical to that of the αA75G/C106V double mutant (2 μM), and the αV173C mutation compensates for the effect of the αA75G mutation so that the αA75G/ C106V/V173C triple mutant has a K_M for $FMNH_2$ of only 0.4 μM. These results show that the overall effect of the multiple mutations is not simply the addition of the contributions of the individual mutations at position α75, α106, and α173 but is the result of complex interactions with the other residues in the active site.

Figure 8 shows that the addition of the αA75G/C106V double mutation, which causes a 4 nm red-shift in the emission spectrum of the wild-type luciferase (λ_{MAX} = 490 nm), also leads to a 4 nm red-shift in the emission spectra of the α173 single point mutants. Addition of the αA75G/C106V double mutation to the αV173T, αV173A, αV173C, and αV173S mutants altered the luciferase emission λ_{MAX} from 494, 498, 500, and 502 nm, respectively, to 498, 502, 504, and 506 nm, respectively, in the triple mutants (Figure 8). Previously, Cline and Hastings (*27*) have isolated five luciferase mutants with very low enzyme activities that display 2−12 nm red-shifts in emission color from the native *V. harveyi* bacteria. Only one mutant (αD113N) previously designated as AK-6 with a 12 nm red-shift in the emission spectrum has been identified by sequence analysis (*28*). The carboxylate side chain of αAsp113 is in a particularly polar microenvironment proximal to the catalytic imidazole group of αHis44 (*1*, *2*, *6*). In the proposed model, the side chains of both αAsp113 and αHis44 on the surface of the active site cavity intercept the boundary between the isoalloxazine chromophore and the aldehyde binding site (*9*). The αD113N mutation could alter the electronic nature of the reaction site near the position 4a on the *si*-face of the isoalloxazine chromophore. This notion is in line with the debilitating effects associated with several αAsp 113 mutations, which significantly decrease the reaction rate and enzyme activity (*28*). In contrast, the αA75G/C106V/ V173A and αA75G/C106V/V173C triple mutations, which have 12 and 14 nm red-shifts, respectively, in emission spectrum, maintain relatively high activities as compared to that of the wild type luciferase. The complementation of these proximal side chains in the three-dimensional structure and the additive effects on shifting the emission spectra without loss of activity provide a good basis to redesign bacterial luciferases to emit light of different colors.

DISCUSSION

Shifting the Color of Bacterial Bioluminescence. In the luciferase-catalyzed reaction, light emission occurs as the chromophore redistributes the high-energy electrons in the extended π-orbitals to the stable state and discharges the stored potentials in the form of a photon. The redistribution of high-energy electrons over conjugated π-orbitals on a light-emitting chromophore is dependent on the chromophore-binding microenvironment. As a result, alteration in the chromophore-binding microenvironment can modulate the energy levels of the conjugated π-orbitals, change the redistribution of the high-energy electrons, and alter the emission color. Examples of bioluminescence color change upon mutation of luciferases include those that utilize coelenterazine and firefly luciferin as substrates.

Coelenteramide, which is the product of the coelenterazine substrate and the light emitter in the calcium-regulated photoprotein, can exist in at least four different high-energy states (each with its own distinct emission color). The probability of occupying any one of these excited states depends on the localization of the single negative charge at one of the three electronegative functional groups in the conjugated π-orbitals of coelenteramide (*29*, *30*). Structure−function studies involving luciferase−coelenterazine interactions reveal that the replacement of a Trp residue by Phe destabilizes the negative charge at the 6-phenylic oxygen of coelenteramide by altering the hydrogen bonding network in the coelenteramide binding site (*30*−*32*). Consequently, this Trp → Phe mutation increases the population of the high-energy chromophore in the neutral form of the coelentera-

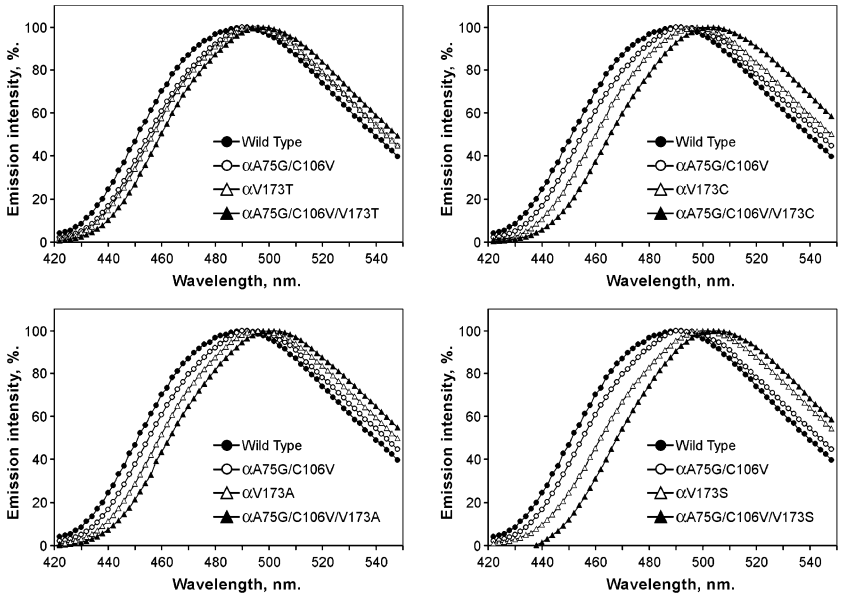

FIGURE 8: Luminescence emission wavelength scans of the mutants, wild-type, and αA75G/C106V double mutants. All the emission spectra were obtained at 5 nm emission (EM) band-pass. Each panel shows that the resulting spectral displacement of the triple mutant is the sum of the differences of the αV173 single point mutation and the αA75G/C106V double mutation from the wild-type.

mide excited-state thus shifting the color of bioluminescence from blue to violet (*30*, *33*, *34*).

In the case of bioluminescence systems that utilize firefly luciferin as substrate, different species of luciferases emit light at wavelengths that range from green (λ_{MAX} ~530 nm) to red (λ_{MAX} ~635 nm) from the common light emitter, oxyluciferin anion (*35*). Although the three-dimensional structure of the oxyluciferin bound firefly luciferase has not been determined (*36*, *37*), a model of the oxyluciferin in complex with the crystal structure of *Photinus pyralis* firefly luciferase has been constructed (*38*). Indeed, mutations of the residues in the proposed oxyluciferin binding site affect the color of bioluminescence emission (*35*, *38*−*41*). However, in few cases, color changes also arise from the mutations located in the outer shell region of luciferase structure, which are believed to weaken the coordination of the bound chromophore by interfering with the assembly of the wild type active site (*42*−*45*).

Unlike the luciferase systems employing the energized reaction products (coelenteramide and oxyluciferin) as light emitters, the postulated light emitter in the bacterial bioluminescence system is a high energy intermediate, C4a−hydroxyFMNH, which decomposes to FMN and water as the final step in the light emission pathway (*46*−*48*). On the basis of our proposed model (*9*), the emitter would project the C4a−hydroxyl moiety toward the aldehyde binding site on the *si*-face of the isoalloxazine chromophore (Figure 2). The induced red-shifts arising from mutations at positions α106 and α173 in bacterial luciferase are most likely the result of alterations in the effective dielectric constants experienced by the flavin isoalloxazine. It has been demonstrated that the enzyme-bound flavin (either in the reduced or oxidized state) is rigidly bound in the active site with little vibrating motion (*21*), providing a strong indication that the energized C4a−hydroxyFMNH chromophore should also be rigidly anchored in luciferase. The altered dielectric field as a result of the mutations (at position α106 and α173) introduced immediately next to the isoalloxazine chromophore can also effectively weaken the binding rigidity of the flavin excited state leading to (1) increased frequency of collision between flavin and nearby molecular anchors, (2) quenching of the excited-state energy in the course of molecular motion, (3) alteration of the density distribution of high-energy electrons on the chromophore, and (4) generating higher populations of the excited chromophore in the low-energy vibrational state, conseqeuently shifting the bioluminescence emission spectrum to longer wavelengths. Nevertheless, the additive effect of color shifts arising from mutations at both positions shows that the disturbance of the electron distribution over the conjugated π-orbitals of flavin is cumulative. These results would also suggest that larger emission shifts in bacterial luciferase can be engineered by combining selected mutations that accommodate the chromophore of the C4a−hydroxyFMNH excited state so that activity is maintained.

Validity of the Luciferase−*Flavin Complex Model.* The effects of the mutations on αVal173 have demonstrated that a compact hydrophobic side chain, preferably bifurcated at the β-carbon, is needed at this position to maintain high affinity for the flavin substrate and retain high functional efficiency of luciferase. Changes in saturation of luciferase with the aldehyde substrate upon mutation of αVal173 were found to be primarily correlated to destabilization of the enzyme-bound C4a−hydroperoxyflavin intermediate, suggesting that all functional changes caused by mutation of αVal173 can be accounted for by the direct interaction of αVal173 with the flavin moiety. This specific luciferase−flavin interaction was further supported by introduction of Cys at position α173 in the αA75G/C106V double mutant leading to inhibition by secondary aldehyde binding likely via a thiol hemi-acetal linkage with αCys173 and blockage of the flavin binding site; the same inhibition as occurs in luciferases containing αCys106 (*26*). This result supports the proposed model (Figure 2) with αCys106 and αVal173 being parallel to each other and forming a common surface for binding the *re*-face of the isoalloxazine ring; secondary aldehyde binding via a thiol hemi-acetal linkage with a Cys

residue at either location would be expected to block flavin binding.

The strongest and most direct proof for binding of the 7,8-dimethylbenzene moiety of the isoalloxazine ring to αVal173 comes from the shifts in emission color on the introduction of polar but not hydrophobic residues at position α173. Such shifts were not related to any changes in the kinetic properties but only depended on the polarity of the microenvironment created by the mutation at this position. This result supports direct contact of the amino acid side chain at position α173 with the flavin ring as any potential changes in color emission arising indirectly via conformational changes should also correlate to a reasonable extent with changes in kinetic properties. Moreover, most mutations in active sites affecting the color of emission of light occur by changes in the polarity of the microenvironment in close contact with the bound chromophore (*35*, *38*−*41*); only in a few instances has it been suggested that mutations at a distance affect the color of light emission (*42*−*45*).

An important property of some of the mutants in this study was the retention of a relatively high level of activity coupled with a shift (4−16 nm) in the emission color. Although a previously study recognized several luciferase mutants with 2−12 nm red-shifts in the emission spectra, only one mutant αD113N was identified with relatively low activity (*27*, *28*). We have now purified this mutant to homogeneity and found that it has a specific activity of only 0.05% that of wild type luciferase (unpublished data). By coupling mutations at position α173 and position α106 and changing the binding microenvironment of the flavin ring even further, larger red-shifts (up to 16 nm) were generated with, in some cases, even a gain of activity. The relatively higher activity (>10% of wild-type activity) of these mutants containing single and multiple mutations supports the role of these residues as a binding platform for the isoalloxazine chromophore. These studies provide strong verification of the proposed interaction of luciferase and flavin in the active site of bacterial luciferase as well as provide the experimental basis for engineering bacterial luciferases catalyzing the emission of light of a different color and still retaining high functional efficiency.

REFERENCES

1. Fisher, A. J., Raushel, F. M., Baldwin, T. O., and Rayment, I. (1995) Three-dimensional structure of bacterial luciferase from *Vibrio harveyi* at 2.4 Å resolution, *Biochemistry 34*, 6581−6586.
2. Fisher, A. J., Thompson, T. B., Thoden, J. B., Baldwin, T. O., and Rayment, I. (1996) The 1.5 Å resolution crystal structure of bacterial luciferase in low salt conditions, *J. Biol. Chem. 271*, 21956−21968.
3. Cline, T. W., and Hastings, J. W. (1972) Mutationally altered bacterial luciferase. Implications for subunit functions, *Biochemistry 11*, 3359−3370.
4. Chen, L. H., and Baldwin, T. O. (1989) Random and site-directed mutagenesis of bacterial luciferase: Investigation of the aldehyde binding site, *Biochemistry 28*, 2684−2689.
5. Li, Z., and Meighen, E. A. (1995) Tryptophan 250 on the α subunit plays an important role in flavin and aldehyde binding to bacterial luciferase. Effects of W → Y mutations on catalytic function, *Biochemistry 34*, 15084−15090.
6. Huang, S., and Tu, S. C. (1997) Identification and characterization of a catalytic base in bacterial luciferase by chemical rescue of a dark mutant, *Biochemistry 36*, 14609−14615.
7. Moore, C., Lei, B., and Tu, S. C. (1999) Relationship between the conserved α subunit arginine 107 and effects of phosphate on the activity and stability of *Vibrio harveyi* luciferase, *Arch. Biochem. Biophys. 370*, 45−50.
8. Lin, L. Y., Sulea, T., Szittner, R., Kor, K., Purisima, E. O., and Meighen, E. A. (2002) Implications of the reactive thiol and the proximal nonproline *cis*-peptide bond in the structural and function of *Vibrio harveyi* luciferase, *Biochemistry 41*, 9938−9945.
9. Lin, L. Y., Sulea, T., Szittner, R., Vassilyev, V., Purisima, E. O., and Meighen, E. A. (2001) Modeling of the bacterial luciferase−flavin mononucleotide complex combining flexible docking with structure−activity data, *Protein Sci. 10*, 1563−1571.
10. Meighen, E. A., and MacKenzie, R. E. (1973) Flavine specificity of enzyme−substrate intermediates in the bacterial bioluminescent reaction. Structural requirements of the flavine side chain, *Biochemistry 12*, 1482−1491.
11. Gunsalus-Miguel, A., Meighen, E. A., Nicoli, M. Z., Nealson, K. H., and Hastings, J. W. (1972) Purification and properties of bacterial luciferases, *J. Biol. Chem. 247*, 398−404.
12. Gill, S. C., and von Hippel, P. H. (1989) Calculation of protein extinction coefficients from amino acid sequence data, *Anal. Biochem. 182*, 319−326.
13. Hastings, J. W., Baldwin, T. O., and Nicoli, M. Z. (1978) Bacterial luciferase: assay, purification, and properties, *Methods Enzymol. 57*, 135−152.
14. Meighen, E. A., and Hastings, J. W. (1971) Binding site determination from kinetic data. Reduced flavin mononucleotide binding to bacterial luciferase, *J. Biol. Chem. 246*, 7666−7674.
15. Mitchell, G. W., and Hastings, J. W. (1971) A stable, inexpensive, solid-state photomultiplier photometer, *Anal. Biochem. 39*, 243−250.
16. Michaliszyn, G. A., Wing, S. S., and Meighen, E. A. (1977) Purification and properties of a NAD(P)H: Flavin oxidoreductase from the luminous bacterium, *Beneckea harveyi*, *J. Biol. Chem. 252*, 7495−7499.
17. Hastings J. W., and Gibson, Q. H. (1963) Intermediates in the bioluminescent oxidation of reduced flavin mononucleotide, *J. Biol. Chem. 238*, 2537−2554.
18. Eberhard, A., and Hastings, J. W. (1972) A postulated mechanism for the bioluminescence oxidation of reduced flavin mononucleotide, *Biochem. Biophys. Res. Commun. 47*, 348−353.
19. Paquatte, O., and Tu, S. C. (1989) Chemical modification and characterization of the α cysteine 106 at the *Vibrio harveyi* luciferase active center, *Photochem. Photobiol. 50*, 817−825.
20. Vervoort, J., Muller, F., Lee, J., van der Berg, W. A. M., and Moonen, C. T. W. (1986) Identifications of the true carbon-13 nulcear magnetic resonance spectrum of the stable intermediate II in bacterial luciferase, *Biochemistry 25*, 8062−8067.
21. Vervoort, J., Muller, F., O'Kane, D. J., Lee, J., and Bacher, A. (1986) Bacterial luciferase: A carbon-13, nitrogen-15, and phosphorus-31 nuclear magnetic resonance investigation, *Biochemistry 25*, 8067−8075.
22. Xi, L., Cho, K. W., Herndon, M. E., and Tu, S. C. (1990) Elicitation of an oxidase activity in bacterial luciferase by site-directed mutation of a noncatalytic residue, *J. Biol. Chem. 265*, 4200−4203.
23. Abu-Soud, H. M., Clark, A. C., Francisco, W. A., Baldwin, T. O., and Raushel, F. M. (1993) Kinetic destabilization of the hydroperoxyflavin intermediate by site-directed modification of the reactive thiol in bacterial luciferase, *J. Biol. Chem. 268*, 7699−7706.
24. Valkova, N., Szittner, R., and Meighen, E. A. (1999) Control of luminescence decay and flavin binding by the luxA carboxyl-terminal regions in chimeric bacterial luciferases, *Biochemistry 38*, 13820−13828.
25. Mitchell, G., and Hastings, J. W. (1969) The effect of flavin isomers and analogues upon the color of bacterial bioluminescence, *J. Biol. Chem. 244*, 2572−2576.
26. Lei, B., Cho, K. W., and Tu, S. C. (1994) Mechanism of aldehyde inhibition of *Vibrio harveyi* luciferase. Identification of two aldehyde sites and relationship between aldehyde and flavin binding, *J. Biol. Chem. 269*, 5612−5618.
27. Cline, T. W., and Hastings, J. W. (1974) Mutated luciferases with altered bioluminescence emission spectra, *J. Biol. Chem. 249*, 4668−4669.
28. Baldwin, T. O., Chen, L. H., Chlumsky, L. J., Devine, J. H., Johnston, T. C., Lin, J.-W., Sugihara, J., Waddle, J. J., and Ziegler, M. M. (1987) Structural analysis of bacterial luciferase, in *Flavins and Flavoproteins* (Edmondson, D. E., and McCormick, D. B., Eds.) pp 621−631, Walter de Gruyter & Co., Berlin.
29. Shimomura, O., and Teranishi, K. (2000) Light-emitters involved in the luminescence of coelenterazine, *Luminescence 15*, 51−58.

30. Deng, L., Vysotski, E. S., Liu, Z. J., Markova, S. V., Malikova, N. P., Lee, J., Rose, J., and Wang, B. C. (2001) Structural basis for the emission of violet bioluminescence from a W92F obelin mutant, *FEBS Lett. 506*, 281−285.
31. Head, J. F., Inouye, S., Teranishi, K., and Shimomura, O. (2000) The crystal structure of the photoprotein aequorin at 2.3 Å resolution, *Nature 405*, 372−376.
32. Liu, Z. J., Vysotski, E. S., Chen, C. J., Rose, J. P., Lee, J., and Wang, B. C. (2000) Structure of the Ca^{2+}-regulated photoprotein obelin at 1.7 Å resolution determined directly from its sulfur substrate, *Protein Sci. 9*, 2085−2093.
33. Ohmiya, Y., Ohashi, M., and Tsuji, F. I. (1992) Two excited states in aequorin bioluminescence induced by tryptophan modification, *FEBS Lett. 301*, 197−201.
34. Vysotski, E. S., Liu, Z. J., Markova, S. V., Blinks, J. R., Deng, L., Frank, L. A., Herko, M., Malikova, N. P., Rose, J. P., Wang, B. C., and Lee, J. (2003) Violet bioluminescence and fast kinetics from W92F obelin: structure-based proposals for the bioluminescence triggering and the identification of the emitting species, *Biochemistry 42*, 6013−6024.
35. Wood, K. V. (1995) The chemical mechanism and evolutionary development of beetle bioluminescence, *Photochem. Photobiol. 62*, 662−675.
36. Conti, E., Franks, N. P., and Brick, P. (1996) Crystal structure of firefly luciferase throws light on a superfamily of adenylate-forming enzymes, *Structure 4*, 287−298.
37. Franks, N. P., Jenkins, A., Conti, E., Lieb, W. R., and Brick, P. (1998) Structural basis for the inhibition of firefly luciferase by a general anesthetic, *Biophys. J. 75*, 2205−2211.
38. Branchini, B. R., Magyar, R. A., Murtiashaw, M. H., Anderson, S. M., Helgerson, L. C., and Zimmer, M. (1999) Site-directed mutagenesis of firefly luciferase active site amino acids: a proposed model for bioluminescence color, *Biochemistry 38*, 13223−13230.
39. Branchini, B. R., Magyar, R. A., Murtiashaw, M. H., Anderson, S. M., and Zimmer, M. (1998) Site-directed mutagenesis of histidine 245 in firefly luciferase: a proposed model of the active site, *Biochemistry 37*, 15311−15319.
40. Branchini, B. R., Magyar, R. A., Murtiashaw, M. H., and Portier, N. C. (2001) The role of active site residue arginine 218 in firefly luciferase bioluminescence, *Biochemistry 40*, 2410−2418.
41. Viviani, V. R., Uchida, A., Viviani, W., and Ohmiya, Y. (2002) The influence of Ala243 (Gly247), Arg215, and Thr226 (Asn230) on the bioluminescence spectra and pH-sensitivity of railroad worm, click beetle, and firefly luciferases, *Photochem. Photobiol. 76*, 538−544.
42. Kajiyama, N., and Nakano, E. (1991) Isolation and characterization of mutants of firefly luciferase, which produce different colors of light, *Protein Eng. 4*, 691−693.
43. Mamaev, S. V., Laikhter, A. L., Arslan, T., and Hecht, S. M. (1996) Firefly luciferase: alteration of the color of emitted light resulting from substitutions at position 286, *J. Am. Chem. Soc. 118*, 7243−7244.
44. Arslan, T., Mamaev, S. V., Mamaev, N. V., and Hecht, S. M. (1997) Structurally modified firefly luciferase. Effects of amino acid substitution at position 286, *J. Am. Chem. Soc. 119*, 10877−10887.
45. Viviani, V. R. (2002) The origin, diversity, and structure−function relationships of insect luciferases, *Cell. Mol. Life Sci. 59*, 1833−1850.
46. Hastings, J. W., and Nealson, K. H. (1977) Bacterial bioluminescence, *Annu. Rev. Microbiol. 31*, 549−595.
47. Kemal, C., and Bruice, T. C. (1977) Chemiluminescence accompanying the decomposition of 4a-flavin alkyl peroxide. Model studies of bacterial luciferase, *J. Am. Chem. Soc. 99*, 7064−7067.
48. Hastings, J. W. (1996) Chemistries and colors of bioluminescent reactions: a review, *Gene 173*, 5−11.

BI030227H